The 9th European Congress on Computational Methods in Applied Sciences and Engineering
ECCOMAS Congress 2024
3 – 7 June 2024, Lisboa, Portugal

LINEAR STATIC AND FREE VIBRATION OF FUNCTIONALLY GRADED NON-SYMMETRICAL I-SHAPED BEAMS

M.A.R. LOJA[*†], A. CARVALHO[*†] AND I.C.J. BARBOSA[*†]

[*] IDMEC, IST - Instituto Superior Técnico
Universidade de Lisboa
Avenida Rovisco Pais 1, 1049-001 Lisboa, Portugal
www.idmec.tecnico.ulisboa.pt

†
CIMOSM, ISEL, IPL
Instituto Superior de Engenharia de Lisboa
R. Conselheiro Emídio Navarro 1, 1959-007 Lisboa, Portugal
www.cimosm.isel.pt
e-mail: amelia.loja@isel.pt; andre.carvalho@isel.pt ; ines.barbosa@isel.pt

Keywords: Functionally graded materials, Finite element method, Non-symmetrical I-shaped cross-section beams.

Summary. Due to their gradually varying properties, functionally graded materials have been known for their minimization of abrupt stress transitions, enhanced thermal protection in high-temperature environments, and improved durability. However, the study of beam structures made of these materials has mostly been limited to applications with rectangular-shaped cross-section beams. Although these cross-section beams are used, other cross-section beams are common, especially in metallic construction. This work investigates the behaviour of non-symmetrical cross-section beams made of functionally graded materials, specifically concerning their static and dynamic behaviour. In this context, different non-symmetrical cross-sections derived from the doubly-symmetric I-shaped cross-section beam are considered. These beams are modelled by a quadratic hexahedron finite element. The steel beams show in general a more conservative behaviour than their functionally graded counterparts, for the materials' mixtures considered. Complementarily, as expected, the natural frequencies of functionally graded material beams are generally higher than those of steel beams. The stress profiles show a significant influence from the non-symmetrical characteristics of cross-sections.

1 INTRODUCTION

Functionally Graded Materials (FGM) are designed to achieve a gradual properties' distribution over the material structure. FGM are overall heterogeneous composite materials with multi-functional characteristics, with at least two different materials whose volume fraction changes gradually along one or more dimensions [1]. It is this characteristic that gives

FGMs a continuously varying composition and structure over the component or structure volume. Hence, FGMs perform very well in specific applications that require certain desired thermal, mechanical, electrical, or chemical properties [2–6]. Moreover, their gradually changing properties allow for FGMs to have improved thermal properties and residual stress distribution, decreased in-plane and traverse stresses over their thickness, and increased fracture resistance [7]. These characteristics make FGMs interesting materials to study. Several authors proposed theories and methods to analyse FGM. Around 60% of the works published use the Navier's method and the power law is the most used homogenization rule [2, 4]. The use of 3D analysis to study FGMs has been hampered by the high computational effort required, so 2D analyses are mostly used together with higher-order shear deformation theories. Also, the meshless method, an alternative to FEM, does not improve time consumption [8]. Regarding FGM manufacturing, several methods are proposed, with powder metallurgy being thought as the most efficient method [7, 8]. Other authors claim that additive manufacturing improves the production of FGMs at a lower cost. This type of manufacturing is known to be capable of producing intricate designs with great accuracy and wasting less material [3, 9]. Several works consider the analyses of FGM beams. Although a multi-layered approach can be considered, most studies use a continuously single-layer approach to model FGM [9–13], particularly when thin-walled structures are studied [14–16]. Different static studies on beam finite elements based on various displacement theories were performed by Filippi et al. [17] and the main difficulty found by the authors regarded shear stress distributions. Though higher-order beam theories were considered to improve these results, their higher computational cost came as a drawback. Several authors identified this problem and came up with different methods and new finite elements to improve the gradient distribution mode and produce more accurate mechanical properties [18–26]. The study of variable axial loading in FGM beams is investigated by Melaibari et al [27] and its effect on buckling and its mode shapes are analysed. Higher-order shear deformation theory is modified to include shear effects, bending and the rigidity of the beam and is proven to be efficient. The materials' mixture distribution as well as orthotropy have an important effect on buckling. Regarding buckling modes, the major influence was found to be related to the gradation of the material and boundary conditions. Free vibration of FGM beams is investigated by several authors [28-33]. The influence of volume fraction distribution, particularly the power index, is the focus of most of those [28-31]. Refined theories and finite element models are introduced to improve the results arising from dynamic studies on FGM beams [32,33]. The dynamic response on porous FGM beams is a present topic of investigation [34-37], with increased porosity distribution index being a major influence on buckling loads and fundamental frequencies [36]. Most studies on FGM beams consider a rectangular cross-section geometry and different cross-section geometries are not easily found in the literature. This was the main motivation for the authors to investigate I-shaped FGM beams [38]. From the studies performed, it is possible to conclude that several differences are found, in comparison to the behaviour of rectangular-shaped cross-section beams, which fully justifies the interest in proceeding with this topic.

2 MATERIALS AND METHODS

2.1 Beam geometrical configurations

The main objective of this work is to characterize the behaviour of FGM non-symmetrical

beams. To achieve this objective, two configurations derived from the doubly symmetric I-shape beam were considered along with the doubly symmetric one, for comparison reasons. These cross-sectional areas are presented in Figure 1-a), where the height of the beams is H=100mm and the width is W=150mm.

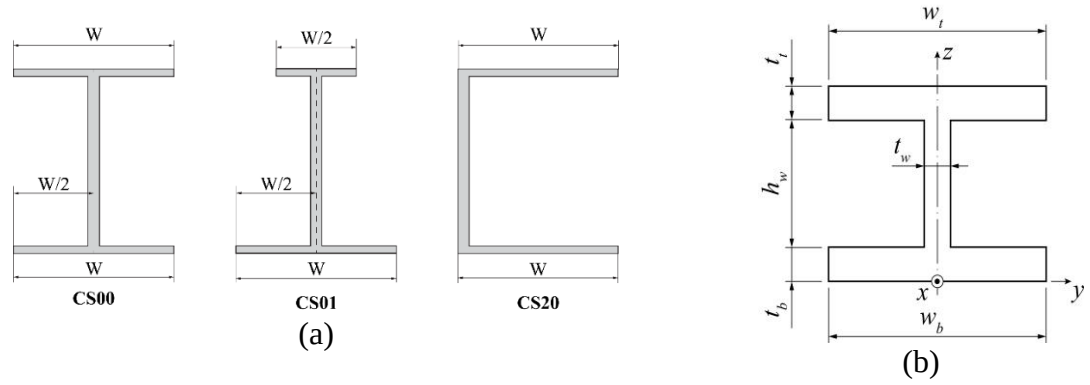

Figure 1: (a) Doubly symmetric I-shape and derived cross-section geometries. (b) Variables that define the beam cross-section geometry

Furthermore, Figure 1-b) shows the axes that were considered in the cross-sections and the variables that define the geometry of the cross-section, such as, w_t, the top flange width, t_w, the web thickness, w_b, the bottom flange width, t_t, the top flange's thickness, h_w, the web height, and t_b, the bottom flange's thickness. It is important to note that the coordinate axes have the origin at the centre point of the bottom of the beam and are oriented as follows: the height of the beam is measured along the z-axis, the width and the length along the y and x-axis.

2.2 Functionally graded material

A FGM is a composite material that involves a gradient micro-structure spatial variation that may occur in different directions [15,25]. The beams considered in this work are made of alumina and steel, whose material properties are presented in Table 1.

Table 1: Material properties

ID	Material	Young's Modulus [GPa]	Poisson's Coefficient	Density [kg/m^3]
A	Alumina	380	0.3	3800
B	Steel	200	0.3	7800

$$V_f = \begin{cases} V_A & 0 \le \frac{z}{H} < z_{min} \\ \dfrac{(V_A - Q_1)\left(\cosh\left(Q_{2_A}\left(\frac{z}{H} - z_{cut_A}\right)\right) - 1\right)}{\cosh\left(Q_{2_A}(z_{min} - z_{cut_A})\right) - 1} + Q_1 & z_{min} \le \frac{z}{H} < z_{cut_A} \\ Q_1 & z_{cut_A} \le \frac{z}{H} < z_{cut_B} \\ \dfrac{(V_B - Q_1)\left(\cosh\left(Q_{2_B}\left(\frac{z}{H} - z_{cut_B}\right)\right) - 1\right)}{\cosh\left(Q_{2_B}(z_{max} - z_{cut_B})\right) - 1} + Q_1 & z_{cut_B} \le \frac{z}{H} < z_{max} \\ V_B & z_{max} < \frac{z}{H} \le 1 \end{cases} \quad (1)$$

To account for the gradation of material along the height of the cross-sectional area, the volume fraction law, V_f, is a function with seven parameters, where z is the thickness coordinate variable; z_{min} and z_{max} are the material saturation limits in the flanges' thickness; z_{cut_A} and z_{cut_B} are the material saturation limits in the web thickness; Q_1 is the minimum quantity of the main material in the web; and Q_{2_A} and Q_{2_B} are controls for the transition between materials. *A* and *B* represent the two materials involved in the gradient. Additionally, the FGM has no porosities.

2.3 Equilibrium equations

The kinematic deformation of the beam, and consequently the stresses' distributions, are based on the description of the movement of a generic point considering its three displacement components (u,v,w) along the 3D Cartesian coordinate system, (x,y,z). Considering the kinematic relations of the Elasticity Theory for small deformations, the strain field characterized by the standard six linear strain components. The materials used are the biphasic FGM mentioned in the previous sub-section, for which a constitutive relation, where the elastic stiffness coefficients depending on the coordinate thickness, applies [39,40]. According to Hamilton's principle:

$$\delta \int_{t0}^{t1} L\, dt = \delta \int_{t0}^{t1} (T - \Pi + \Omega)\, dt = 0 \tag{2}$$

where T is the kinetic energy, Π is the elastic strain energy and Ω stands for the work done by the external forces. To perform a free vibration analysis or a linear static analysis, the mathematical manipulation of this equation will yield, at the element level:

$$(\boldsymbol{K}_e - \omega^2 \boldsymbol{M}_e)\boldsymbol{q}_e = 0 \quad ; \quad \boldsymbol{K}_e \boldsymbol{q}_e = \boldsymbol{f}_e \tag{3}$$

with $\boldsymbol{K}_e$ and $\boldsymbol{M}_e$ standing respectively for the element elastic stiffness matrix and the element mass matrix. The vectors $\boldsymbol{q}_e$ and $\boldsymbol{f}_e$ represent the generalized degrees of freedom vector and the element vector of the surface forces respectively. A Lagrange tri-quadratic element, shown in Figure 2, was used to implement these equations via the finite element method.

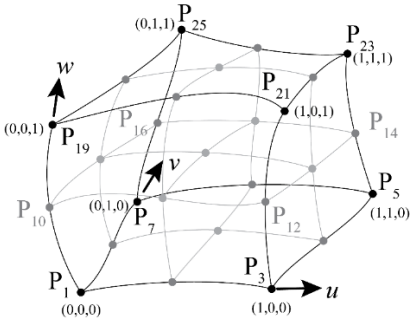

Figure 2: Generic Lagrange tri-quadratic finite element and its local coordinate system.

The solution of these equations extended to the whole discretized domain, is obtained after solving the corresponding reduced equilibrium equations systems.

3 RESULTS AND DISCUSSION

Several studies were performed to investigate the behaviour of FGM non-symmetrical beams

concerning their free vibration responses as well as, maximum static deflections and stresses' profiles. It is important to note that the same material distribution is considered for all FGM beams. This distribution is the one presented in Equation 1 and the distribution parameters used in the volume fraction law for these case studies are the following: z_{min}=6.44%, z_{max}=93.56%, $z_{cut\ A}$=45%, $z_{cut\ B}$=55%, C_1=0, C_{2A}=10%, C_{2B}=10%.

3.1 Maximum displacement analysis

After performing a convergence analysis, the beams with different configurations, under different boundary conditions, were submitted to a uniformly distributed load of 1 kPa, and the maximum static transverse displacement was obtained.

3.1.1 Effect of the cross-sectional area

At first, the effect of the cross-sectional area was considered. The three configurations present in Figure 1 were analysed for a C-C boundary condition. Two aspect ratios were considered, L/H=20 and L/h=5, respectively associated with thin and thick beams. The maximum displacement is presented in Figure 3-a) and 3-b) for the different configurations and aspect ratios. As expected, the thin beams obtained higher maximum deflections. In terms of the cross-sectional area, the configuration closer to the doubly symmetric I-shape cross-section shows smaller deflections and the C-shape cross-section presents the highest deflection. Configuration CS01 performs best in both aspect ratio situations.

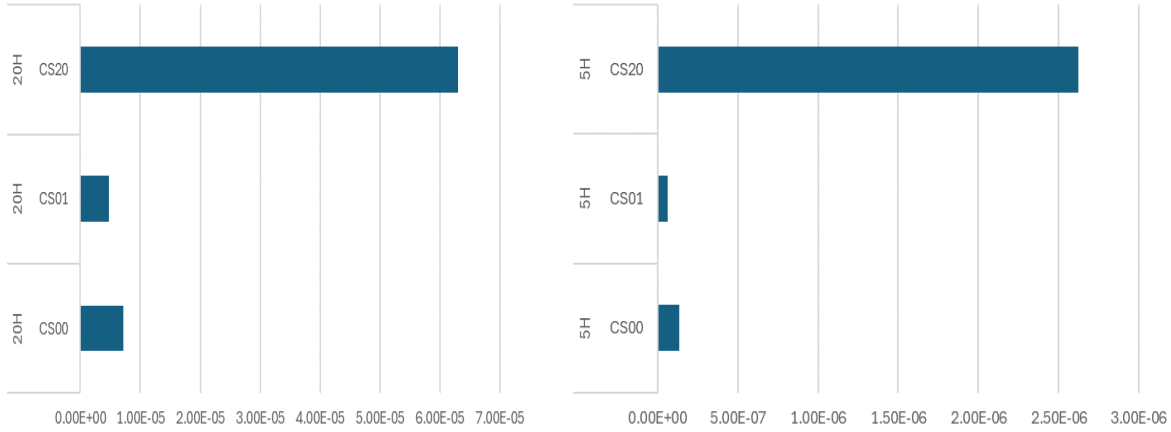

(a) (b)

Figure 3: Maximum static deflection (a) of thin beams (L/H=20), (b) of thick beams (L/H=5).

3.2.2 Effect of the material

The configuration studied was the least symmetric about the vertical axis z, the configuration CS20, as it has proved in the previous study to be the less stiff one. So, the beam was subjected to the C-F boundary condition and an FGM beam, and a steel beam were studied. When thin beams are considered, the maximum displacements, presented in Figures 4-a) and 4-b), show that the FGM beam yields higher deflections than the steel beam, but, for thick beams, the opposite occurs.

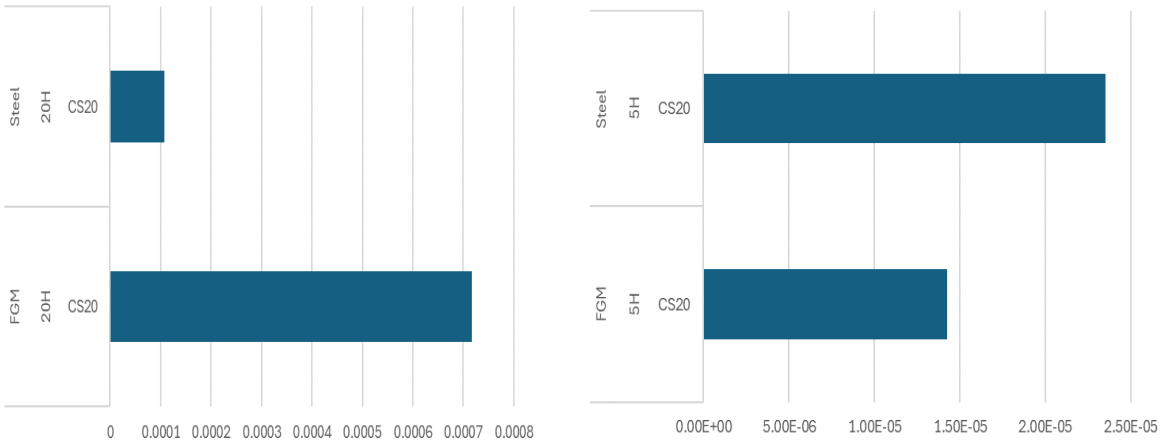

(a) (b)

Figure 4*:* Maximum displacement of CS20 beam, made of different materials (a) L/H=20 (b) L/H=5.

3.2.3 Stresses distributions

The stresses' distributions were studied for different aspect ratios considering three locations along beam length (L/4, L/2, 3L/4).

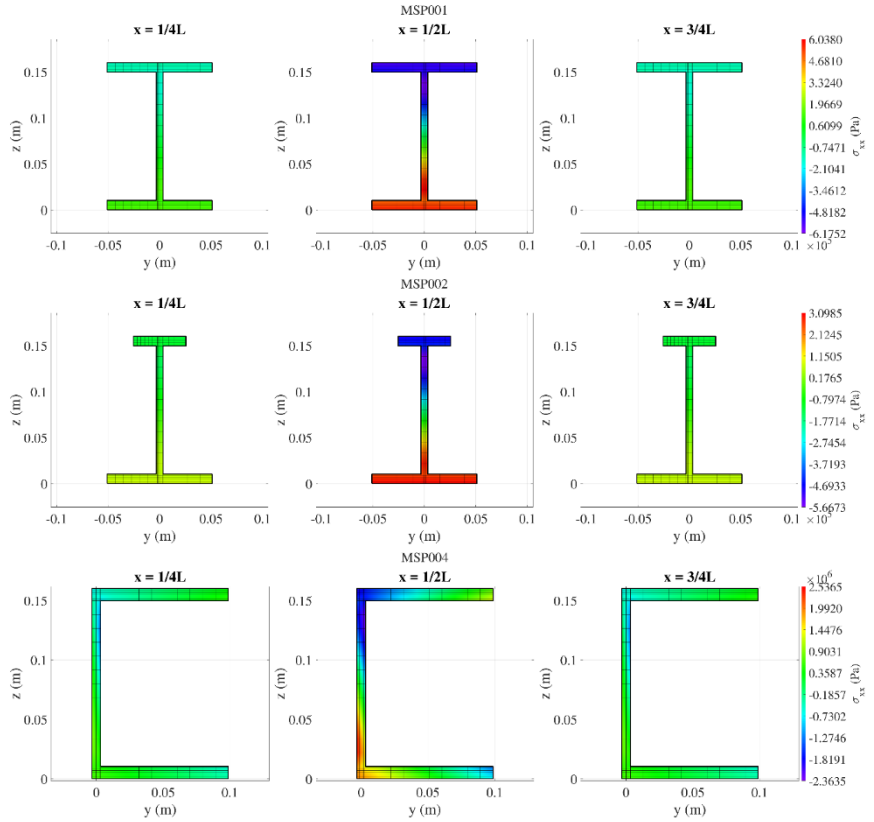

Figure 5*:* Stress distribution σ_{xx} (L/H=20).

For illustrative purposes, the stress along the length of the beam, σ_{xx}, for L/H=20 is shown

in Figure 5. The higher stresses occur at L/2. Configuration CS20 displays a shift in the location of the higher stresses along the y-axis, due to the cross-sectional geometry. Furthermore, these higher stresses occur in the flanges or near the interface between the web and the flange. Other stress components were assessed however they aren't here presented for the sake of brevity. Regarding these cases, note that the stress distribution along the height of the beam (σ_{zz}) and the higher stresses occur in the web, although not symmetric. Regarding the transverse shear stress distribution, τ_{xy}, there is no deviation regarding the z-axis, with higher stresses in the middle height of the web. For the CS20, these higher stresses occur in the inner face of the section and closer to the supports of the beam, instead of the middle length. To further investigate the shear stress distribution, a static analysis of the thick CS20 beam was performed, and it was observed that higher τ_{xy}, stresses developed along the width of the web, reaching the outer side.

3.3 Free vibration analysis

The beams were analysed concerning their free vibration responses and the fundamental frequency was compared for different aspect ratios and boundary conditions. The effect of the material used for the beams was also considered. Considering the aspect ratio, the fundamental frequencies are considerably higher for thick beams (L/H=5), around 20 times higher than thin beams (L/H=20), as may be observed in Figure *6*6.

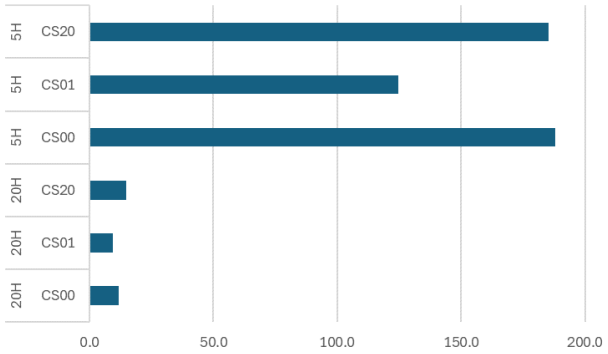

Figure 6: Fundamental frequency of the beams for different aspect ratios.

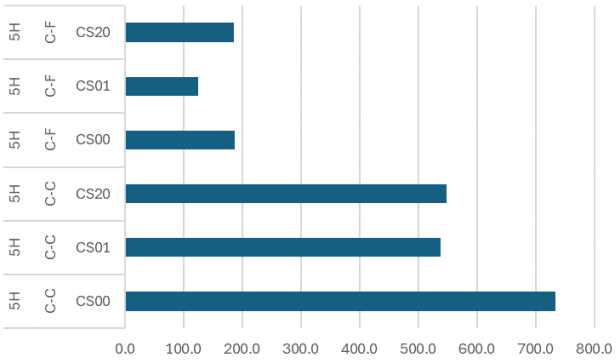

Figure 7: Fundamental frequency of the beams for L/H=5 and different boundary conditions.

Also, thick beams present a different mode behaviour, when compared to thin beams (Figure 7).

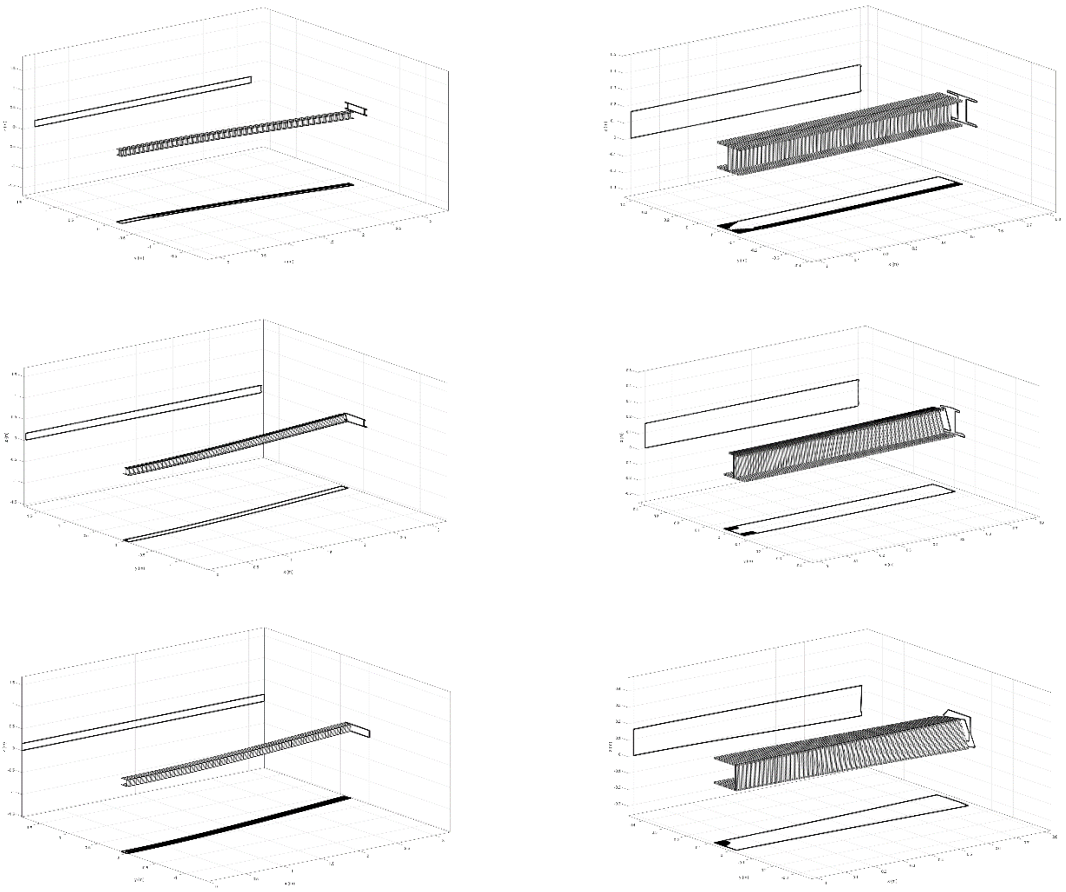

(a) (b)

Figure 8: Fundamental vibration modes for C-F FGM beams with three cross-sections (CS00, CS01, and CS20): (a) for L/H=20, (b) for L/H=5.

When comparing the effects of different boundary conditions, it is confirmed as expected, that double-clamped beams have higher fundamental frequencies than clamped-free beams, as may be observed in Figure 8. By clamping both ends, the stiffness of the beam is greatly increased while the mass remains constant.

In terms of the modes' shapes of the modes, it was found that thicker beams have a more pronounced torsional mode in comparison to the first bending mode in longer beams, where the bending is dominant (Figure 9).

It is also relevant to note, that when considering the shapes of higher-order modes, the frequent presence of local modes on the web and flanges is much more noticeable for shorter beams. For longer beams, the modes are dominated by the full-body bending and torsional mode shapes.

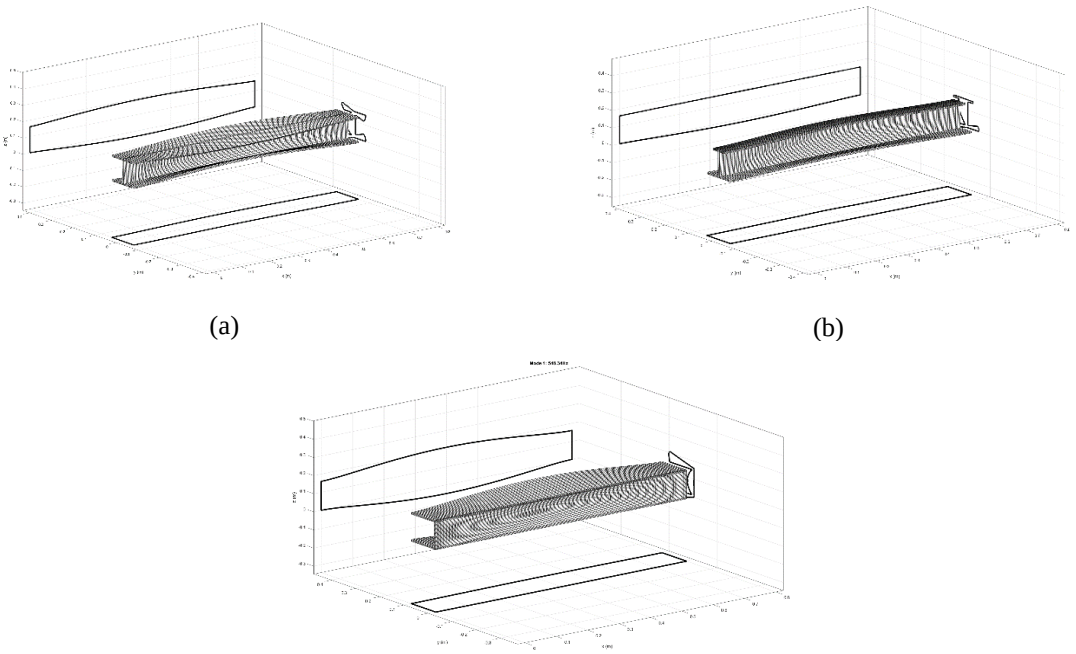

(a) (b)

(c)

Figure 9*:* Fundamental vibration modes for C-C FGM beams with CS00, CS01, and CS20 cross-sections and L/H=5.

12 CONCLUSIONS

The study of FGM beams with non-symmetrical cross-sections was the focus of the present work. A quadratic hexahedron finite element model was used to analyse the doubly symmetrical I-shaped FGM beam, as well as two derived cross-sectional beams. The beams were subjected to a uniformly distributed load and the maximum displacement was obtained. The stress distribution was obtained and compared to the results of a corresponding steel beam. The beams were also studied concerning their free vibration response.

The results showed that for the materials considered, the steel beams present a more conservative behaviour when compared to their FGM counterparts.

The stress distribution is very dependent on the cross-sectional area, showing deviations due to the nonsymmetric cross-section. Also, the CS20 (C-shaped) FGM beam presented higher stresses in the inner wall of the web, not extending to the whole web width. Furthermore, the stress distribution in this FGM beam has a diagonal evolution along the height.

The effect of the length-to-thickness aspect ratio was investigated, and it was found that there is a significant influence on the maximum static displacements and the stress distributions.

Regarding the vibration analysis, natural frequencies were higher for FGM beams than steel beams.

The aspect ratio has an important influence on the fundamental frequencies as these are considerably higher for thick beams. These beams also presented more predominance on the torsional mode shape due to the boundary conditions.

The vibrational modes are significantly affected by the cross-section geometries, while the

material distribution mainly affects the magnitude of the natural frequencies.

REFERENCES

[1] Koizumi, M. "FGM activities in Japan". 1997. *Composites Part B: Engineering*, 28, No.1–4, 1. http://doi.org/10.1016/S1359-8368(96)00016-9.

[2] Sayyad, A.S., and Y. M. Ghugal. 2019. "Modeling and analysis of functionally graded sandwich beams: a review". *Mech Adv Mat Struc*, 26, 1776–1795. http://doi.org/10.1080/15376494.2018.1447178.

[3] Saleh, B., J. Jiang, R. Fathi, T. Al-hababi, Q. Xu, L. Wang, D. Song, and A. Ma. 2020. "30 years of functionally graded materials: An overview of manufacturing methods, applications and future challenges". *Composites Part B: Engineering*, 201, 108376. http://doi.org/10.1016/j.compositesb.2020.108376.

[4] Garg, A., M.-O. Belarbi, H. Chalak, and A. Chakrabarti. 2021. "A review of the analysis of sandwich FGM structures". *Comp Struc*, 258, 113427. http://doi.org/10.1016/j.compstruct. 2020.113427.

[5] Sarkar, L., Saha, S., Samanta, R., Sinha, A., Mandal, G., Biswas, A., and Das, A. 2024. "Recent Progress in CNT-Reinforced Composite and FGM for Multi-functional Space Applications and Future Directions". *J Inst Eng (India): Series D*, *105*(1), 527-541. https://doi.org/10.1007/s40033-023-00465-y

[6] Ogbonna, V., Popoola, A., Popoola, O. and Adeosun, S. 2021. "Recent progress on improving the mechanical, thermal and electrical conductivity properties of polyimide matrix composites from nanofillers perspective for technological applications". *Journal of Polymer Engineering*, *41*(9), 768-787. https://doi.org/10.1515/polyeng-2021-0176

[7] Parihar, R. S., S. G. Setti, and R. K. Sahu. 2018. "Recent advances in the manufacturing processes of functionally graded materials: A review". *IEEE J Selec Topics Quantum Electr*, 25, 309–336. http://doi.org/10.1515/secm-2015-0395.

[8] Kanu, N. J., U.K. Vates, G.K. Singh, and S. Chavan. 2019. "Fracture problems, vibration, buckling, and bending analyses of functionally graded materials: A state-of-the-art review including smart FGMS". *Particulate Sci Tech*, 37, 583–608. http://doi.org/10.1080/02726351. 2017.1410265.

[9] Jayachandiran, G., and Ramamoorthy, M. 2023. Advancements in manufacturing and vibration analysis of functionally graded polymer composites: A review. *Mech Adv Mat and Struc*, 1–20. https://doi.org/10.1080/15376494.2023.2289086

[10] Banks-Sills, L., R. Eliasi, and Y. Berlin. 2002. "Modeling of functionally graded materials in dynamic analyses". *Composites Part B: Engineering*, 33, 7–15.

[11] Kasem, M.M., and K.Y. Maalawi. 2021. "Multiobjective optimization of functionally graded material columns". 323–326. *Inst of Electrical and Electronics Eng Inc*. http://doi.org/10.1109/NILES53778.2021.9600498.

[12] Dastjerdi, F.B., and M. Jabbari. 2022. "Analytical analysis for non-homogeneous two-layer functionally graded material". *Nonlinear Eng*, 11, 598–608. http://doi.org/10.1515/nleng-2022-0258.

[13] He, D., Q. Wang, R. Zhong, and B. Qin. 2023. "Vibration analysis of functionally graded material (FGM) double layered floating raft structure by the spectro-geometric method". *Structures*, 48, 533–550. http://doi.org/10.1016/j.istruc.2022.11.111.

[14] Nguyen, T.T., N. I. Kim, and J. Lee. 2016. “Analysis of thin-walled open-section beams with functionally graded materials”. *Comp Struc*, 138, 75–83. http://doi.org/10.1016/j.compstruct.2015.11.052.

[15] Loja, M.A.R. and J. I. Barbosa. 2020. “In-plane functionally graded plates: A study on the free vibration and dynamic instability behaviours”. *Comp Struc*, 237, No. 4. http://doi.org/10.1016/j.compstruct.2020.111905.

[16] Asiri, S. 2022. “Comparative modal analysis on fishing rod made of functionally graded composite material using finite element análisis”. *J Appl Biomaterials and Functional Materials*, 20, No. 3. http://doi.org/10.1177/22808000221089774.

[17] Filippi, M., E. Carrera, and A. M. Zenkour. 2015. “Static analyses of FGM beams by various theories and finite elements”. *Composites Part B: Engineering*, 72,1–9. http://doi.org/10.1016/j. compositesb.2014.12.004.

[18] Chakraborty, A., S. Gopalakrishnan, and J. N. Reddy. 2003 “A new beam finite element for the analysis of functionally graded materials”. *Int J Mech Sci*, 45, 519–539. http://doi.org/10.1016/S0020-7403(03)00058-4.

[19] Yoon, K., P. S. Lee, and D. N. Kim. 2015. “Geometrically nonlinear finite element analysis of functionally graded 3D beams considering warping effects”. *Comp Struc*, 132, 1231–1247. http://doi.org/10.1016/j.compstruct.2015.07.024.

[20] Correia, F.E.M., Mota, A.F.S., Loja, M.A.R. 2020. “Variable stiffness composites: Optimal design studies”. *J. Comp Sci*, 4(2), article 80. Doi: 10.3390/jcs4020080

[21] Bian, P. L., H. Qing, and T. Yu. 2022. “A new finite element method framework for axially functionally graded nanobeam with stress-driven two-phase nonlocal integral model”. *Comp Struc*, 295. http://doi.org/10.1016/j.compstruct.2022.115769.

[22] Mota, A.F., M. A. Loja, J. I. Barbosa, and M. Vinyas. 2022. “Mechanical behavior of a sandwich plate with aluminum foam core, using an image-based layerwise model”. *Mech Adv Mat Struc*, 29, 4074 – 4095. http://doi.org/10.1080/15376494.2021.1919801.

[23] Luo, Y. 2023. “Voxel-based design and characterization of functionally graded materials”. *Results in Materials*, 17. http://doi.org/10.1016/j.rinma.2023.100375.

[24] Luu, N.G. and T. T. Banh. 2023. “Static, dynamic and stability analysis of multi-dimensional functional graded plate with variable thickness using deep neural network”. Technical report, arXiv.org.

[25] Carvalho, A., T. Silva, M. Loja, and F. Damasio. 2017. “Assessing the influence of material and geometrical uncertainty on the mechanical behavior of functionally graded material plates”. *Mech Adv Mat Struc*, 24, No. 5, 417–426. http://doi.org/10.1080/15376494.2016.1191100.

[26] Yadav, S., S. Damse, S. Pendhari, K. Sangle and A.S. Sayyad. 2022 “Comparative studies between Semi-analytical and shear deformation theories for functionally graded beam under vending”. *Forces in Mechanics* 8, 100111. http://doi.org/10.1016/j.finmec.2022.100111

[27] Melaibari A., R.M. Abo-bakr, S.A. Mohamed, and M.A. Eltaher. 2020. “Static stability of higher order functionally graded beam under variable axial load”. *Alex Eng J* 59, 1661–1675. https://doi.org/10.1016/j.aej.2020.04.012

[28] Li S., Z. Wan, and J. Zhang. 2014. “Free vibration of functionally graded beams based on both classical and first-order shear deformation beam theories”. Appl. Math. Mech. - Engl. Ed., 35(5), 591–606. https://doi.org/10.1007/s10483-014-1815-6

[29] Pradhan K.K., and S. Chakraverty. 2014. “Effects of different shear deformation theories on free vibration of functionally graded beams”. *Int J Mech Sci*, 82, 149–160. http://dx.doi.org/10.1016/j.ijmecsci.2014.03.014

[30] Chaabane, L.A., F. Bourada, M. Sekkal, S. Zerouati, F.Z. Zaoui, A. Tounsi, A. Derras, A.A. Bousahla, and A. Tounsi. 2019. “Analytical study of bending and free vibration responses of functionally graded beams resting on elastic foundation”. *Struc Eng Mech*, 71, No. 2, 185-196. https://doi.org/10.12989/sem.2019.71.2.185

[31] Wu, D., A. Liu, Y. Huang, Y. Huang, Y. Pi, and W. Gao. 2018. “Dynamic analysis of functionally graded porous structures through finite element analysis”. *Eng Struct* 165, 287–301. https://doi.org/10.1016/j.engstruct.2018.03.023

[32] Kouami, K., M. Foudil, D. El Mostafa, and C. Erasmo. 2021. “A finite element approach for the static and vibration analyses of functionally graded material viscoelastic sandwich beams with nonlinear material behavior”. *Comp Struc* 274, 114315. https://doi.org/10.1016/j.compstruct.2021.114315

[33] Boutahar Y., N. Lebaal, and D. Bassir. 2021. “A Refined Theory for Bending Vibratory Analysis of Thick Functionally Graded Beams”. *Mathematics* 9, 1422. https://doi.org/10.3390/math9121422

[34] Chen D., J. Yang, and S. Kitipornchai. 2016. “Free and forced vibrations of shear deformable functionally graded porous beams”. *Int J Mech Sci* 108-109, 14–22. http://dx.doi.org/10.1016/j.ijmecsci.2016.01.025

[35] Wang Y., and D. Wu. 2017. “Free vibration of functionally graded porous cylindrical shell using a sinusoidal shear deformation theory”. *Aero Sci and Tech* 66, 83–91. http://dx.doi.org/10.1016/j.ast.2017.03.003

[36] Chen D., S. Rezaei, P.L. Rosendahl, B.X. Xu, and J. Schneider. 2022. “Multiscale modelling of functionally graded porous beams: Buckling and vibration analyses”. *Eng Struc* 266, 114568. https://doi.org/10.1016/j.engstruct.2022.114568

[37] Zhang, L., Z. Xu, M.Gao, R. Xu, and G. Wang. 2023. “Static, dynamic and buckling responses of random functionally graded beams reinforced by graphene platelets”. *Eng Struc* 291, 116476. https://doi.org/10.1016/j.engstruct.2023.116476

[38] Loja, M.A.R., A. Carvalho, and I.C.J. Barbosa. 2024. “A study on the static behavior of functionally graded I-shaped beams”. *AIMS Mat Sci*, 11, Issue 1: 28-57. https://doi.org/10.3934/matersci.2024002

[39] J. N. Reddy. 2003. *Mechanics of Laminated Composite Plates and Shells*. 2nd ed., CRC Press.

[40] Carvalho, A. 2023. “Study of damping of bare and encased steel I-beams using the thermoelastic model”. *Buildings*, 13, No.12, 2964. https://doi.org/10.3390/buildings13122964